Formation of atmospheres

PhD students: Thomas Lebrun, Arnaud Salvador.

Collaborateurs: Anne Davaille (FAST), Philippe Sarda (GEOPS), Emmanuel Marcq (LATMOS), François Leblanc (LATMOS), Henri Samuel (IPGP), Eric Chassefière (GEOPS), Geneviève Brandeis (IPGP).

Hélène Massol - GEOPS - U. Paris Saclay

GEOPS GEOSCIENCES PARIS-SACLAY   université PARIS-SACLAY

Outline

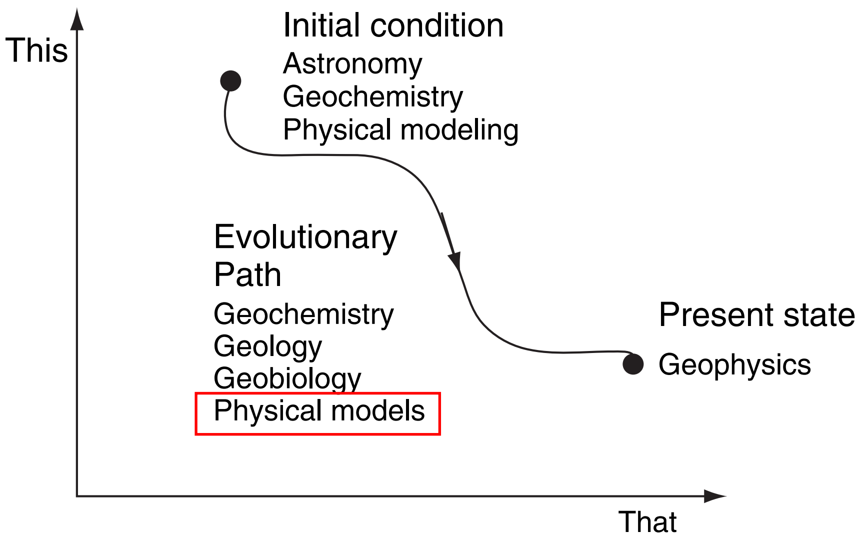

Figure 1 Conceptual view of Earth evolution, identifying the three crucial elements (the initial condition, the evolution path, and the present state) and the sciences that contribute to their understanding. The axes are unimportant, since the diagram is merely a 2-D slice of a multidimensional phase space. They might represent temperature or composition, for example.

Stevenson, 2014

- Introduction / constraints
- Heat and volatile transfer during MO Phase
- Examples, results and applications to exo-planets

Introduction / constraints: primary atmosphere

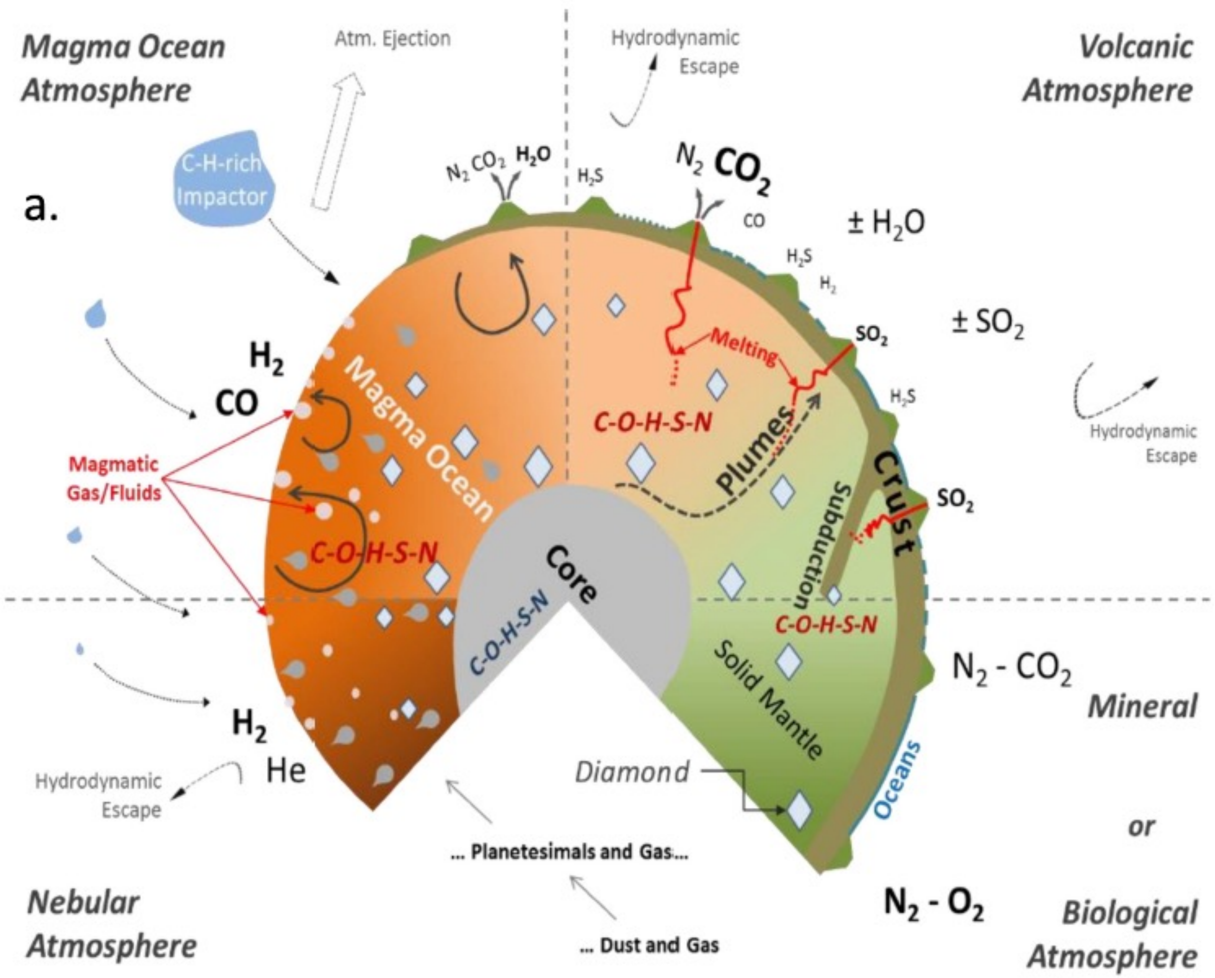

Gaillard et al., 2021

Introduction / constraints: chronology of events

Dissipation of gas in the protoplanetary gas confirmed around
10 My by datation using short lived Pd-Ag system on Iron meteorites (*Hunt et al., 2022*)

Constraints on the time of formation of Earth
Hf-W + U pb: ~30 – 100 My and Mars : 1 – 10 My measured on martian meteorites

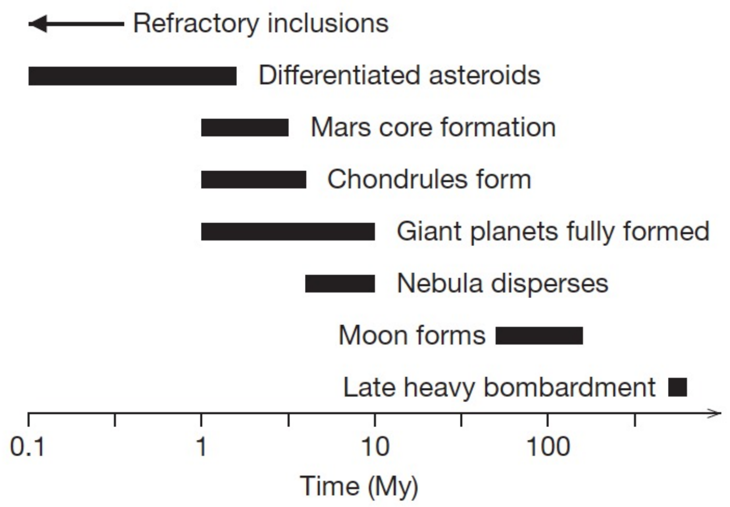

Figure 1 The timing of events in the early Solar System (Data and models: Dauphas and Pourmand, 2011; Hutcheon et al., 2009; Movshovitz et al., 2010; Qin et al., 2008; Sung et al., 2009; Touboul et al., 2007).

Chambers, 2014

Introduction / constraints: different types of meteorites

Solidified magma

From core-mantle boundary

Fragments of planetary cores

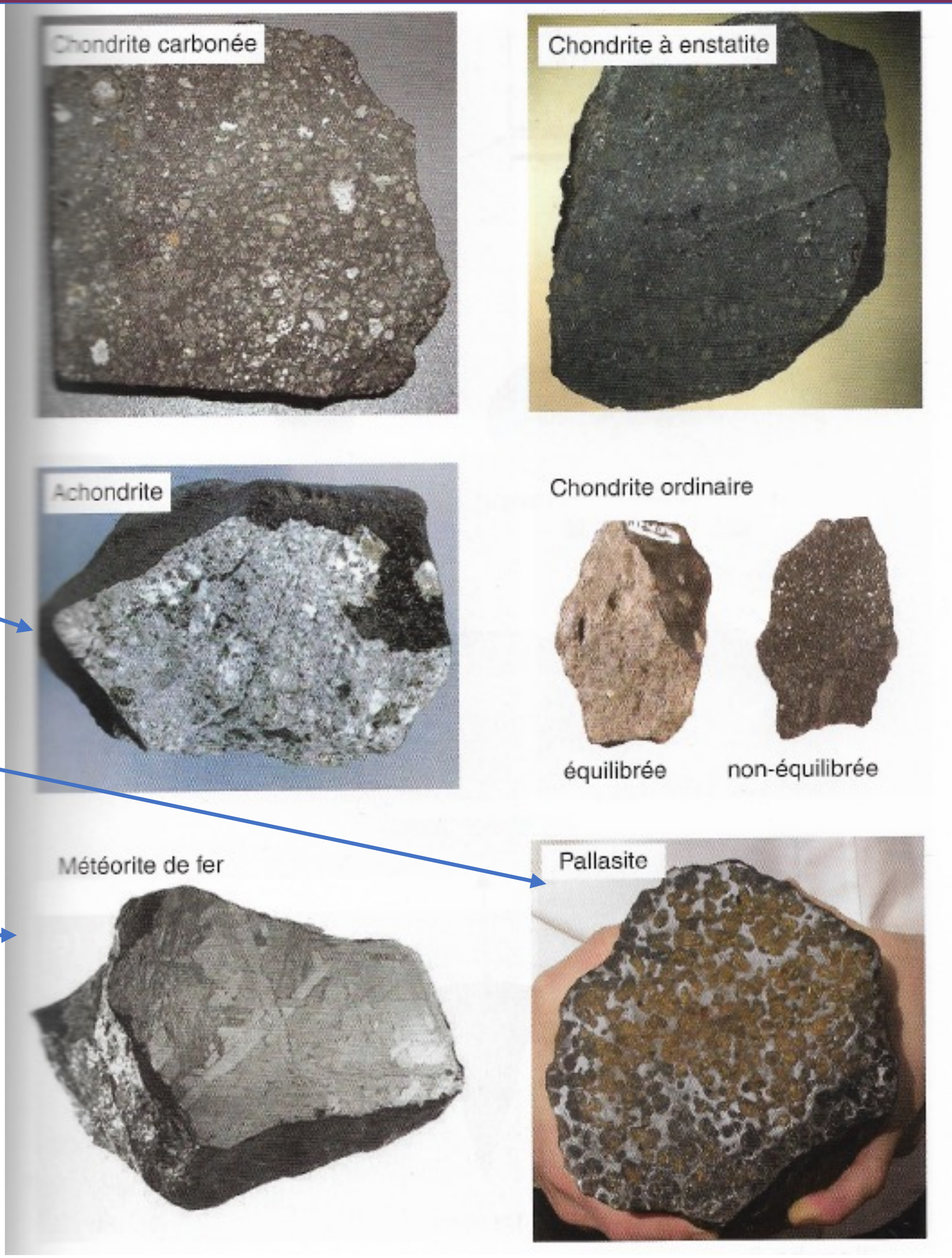

Planétologie, Sotin et al., Dunod

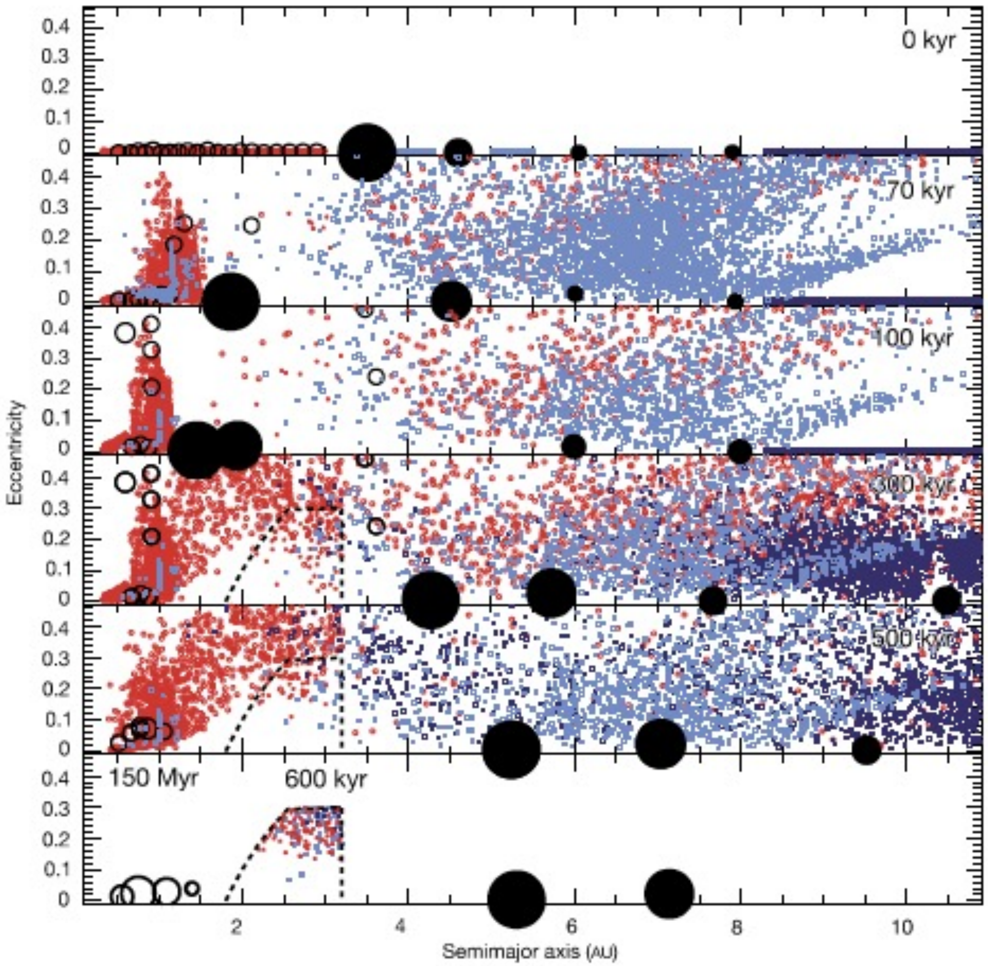

Fig. 3 Figure from Walsh et al. (2011) showing a simulation of the Grand Tack scenario. The *top three panels*

These ages compatible with accretion models

O Brien, 2018

Introduction / constraints:

Super Earth less than 20 $M_\oplus$

Diversity in H content

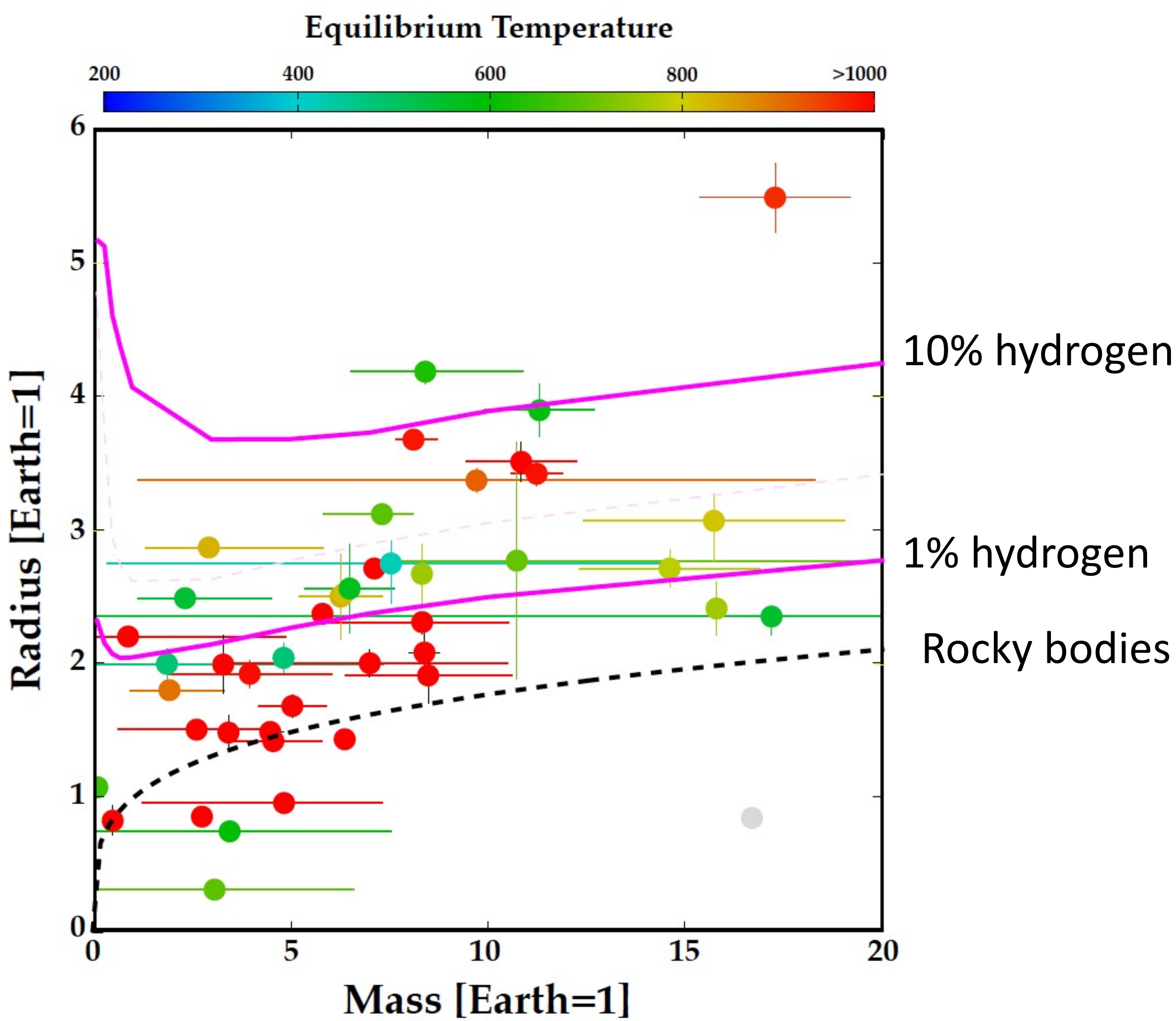

Massol, 2016 based on Lopez and Fortney, 2014

Introduction / constraints:

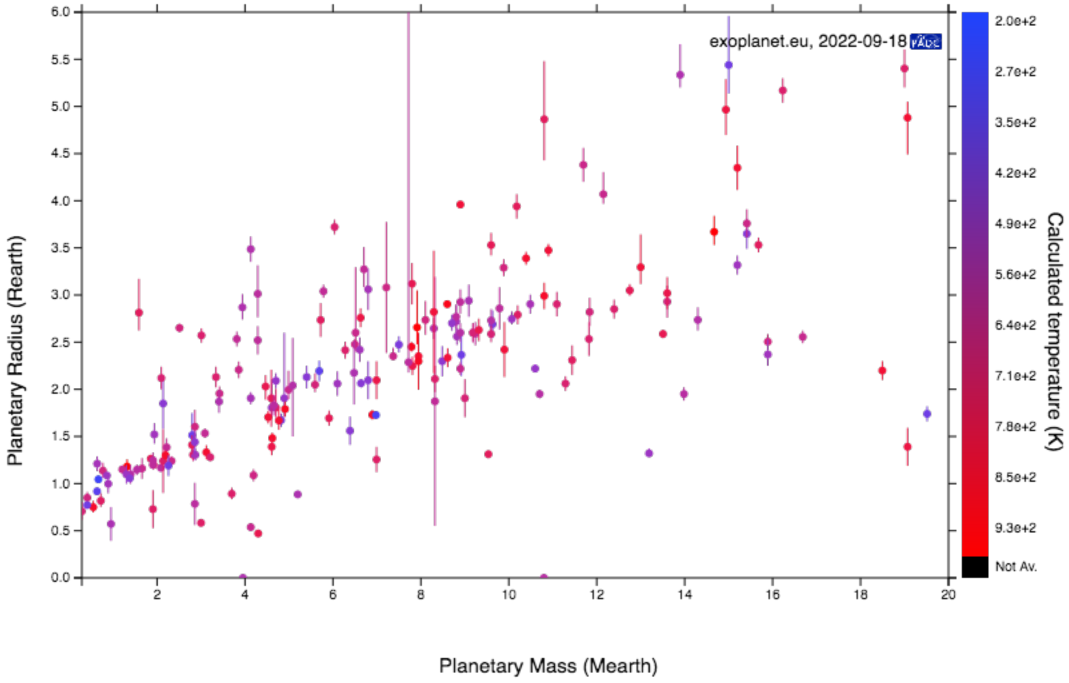

Cause of magma ocean

- Blanketting by a dense primary atmosphere
- Impacts
- Radiogenic elements (Al26)

Image Credit: NASA/JPL-Caltech

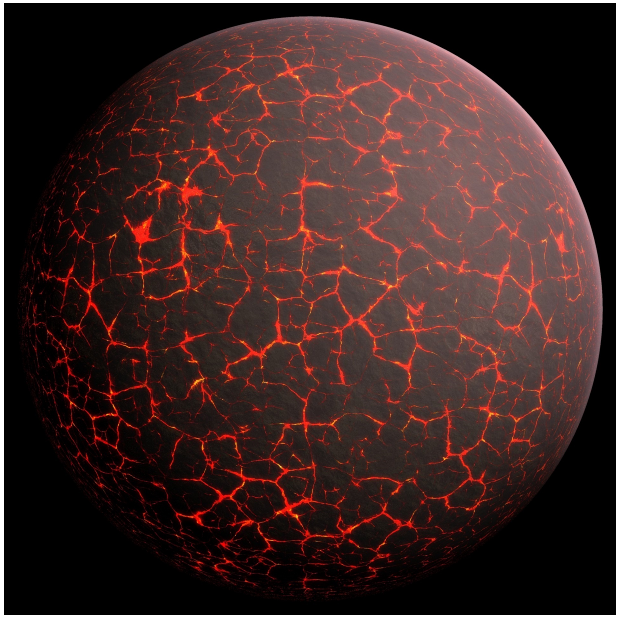

By PublicDomainPictures - http://pixabay.com/en/mercury-venus-earth-mars-jupiter-163610/, CC0, https://commons.wikimedia.org/w/index.php?curid=37984303

Introduction / constraints: Magma oceans

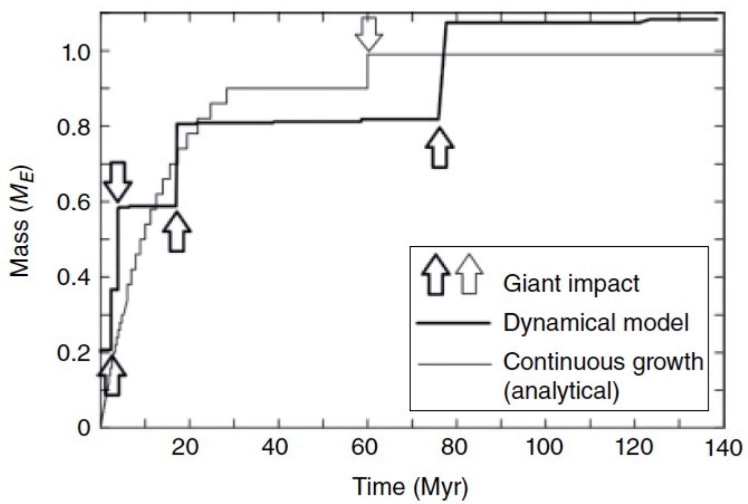

Figure 5.1 Bold line shows a typical growth curve from an N-body simulation [run2a of *Raymond et al.*, 20(arrows indicate giant impacts. The thin line assumes growth at an exponentially decaying rate (equation 5.4) wi timescale τ of 10 Myr and a later final Moon-forming impact. Exponential growth models with longer e-folding timescales have been used to reproduce the Hf-W and U-Pb isotope systematics of the Earth [*Halliday*, 2004; *Rudge et al.*, 2010] under the assumption of incomplete re-equilibration during impacts (Section 5.2.4.1). M_E is one Earth mass.

Nimmo & Kleine 2015

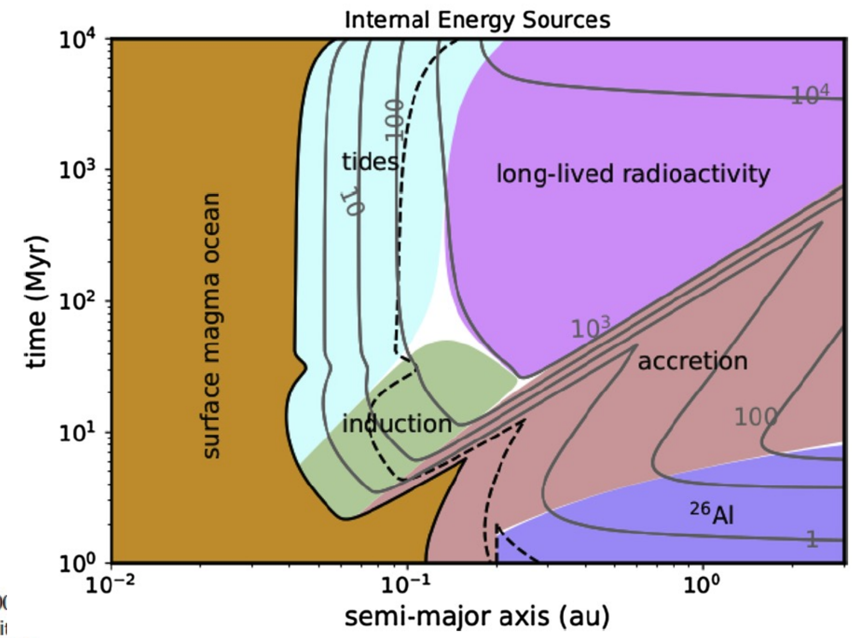

Chao, 2021

Introduction / constraints: Magma oceans

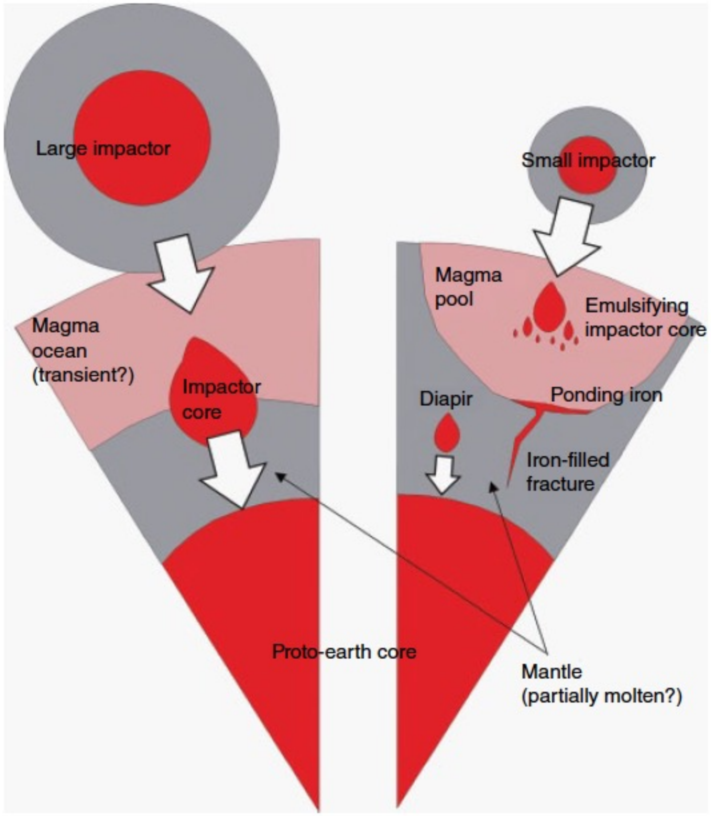

Nimmo & Kleine 2015

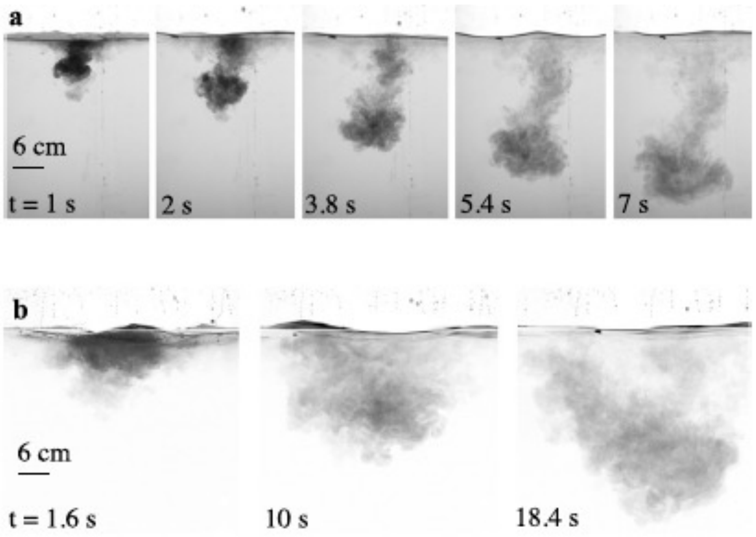

Fig. 3. Late-time thermal stage following the impact shown in Fig. 2. (a) Low impact Froude number, $Fr \simeq 6$, $U \simeq 1.3$ m s^{-1}. (b) High impact Froude number, $Fr \simeq 100$, $U \simeq 5.4$ m s^{-1}. In both experiments $P \simeq 0.02$ and the impactor radius $R \simeq 3$ cm. The experiments in (a) and (b) correspond to supplementary movies S1 and S2, respectively.

Landeau et al., 2021

Certaines petites planètes sans atmospheres primitives vont pouvoir former une atmosphere secondaire Par dégazage.

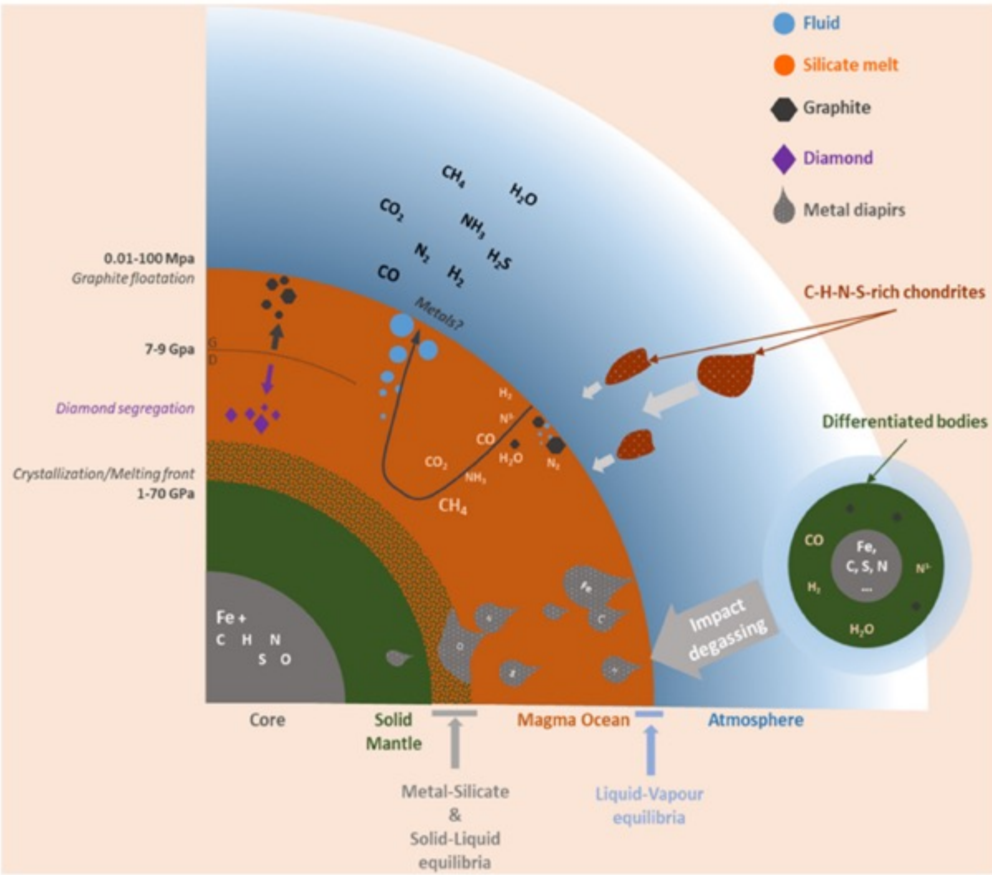

Gaillard et al. 2022

$$\underset{\text{molten alloy}}{Fe} + 1/2\ O_2 \Longleftrightarrow \underset{\text{molten silicate}}{FeO}$$

Hirschmann, 2022

IW: f_{O2}

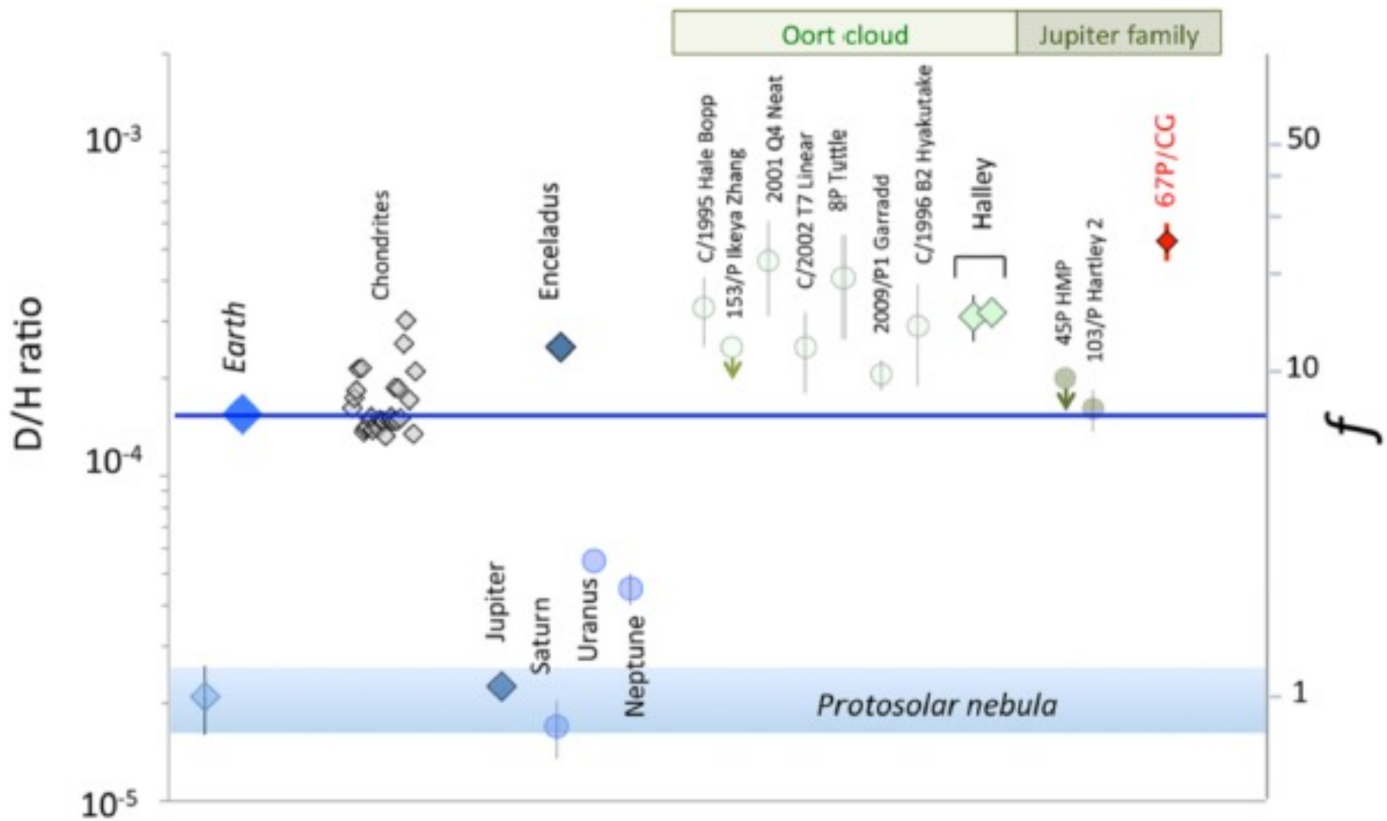

Altwegg et al., 2015

CometWatch - NavCam images, ESA 7/7/2015

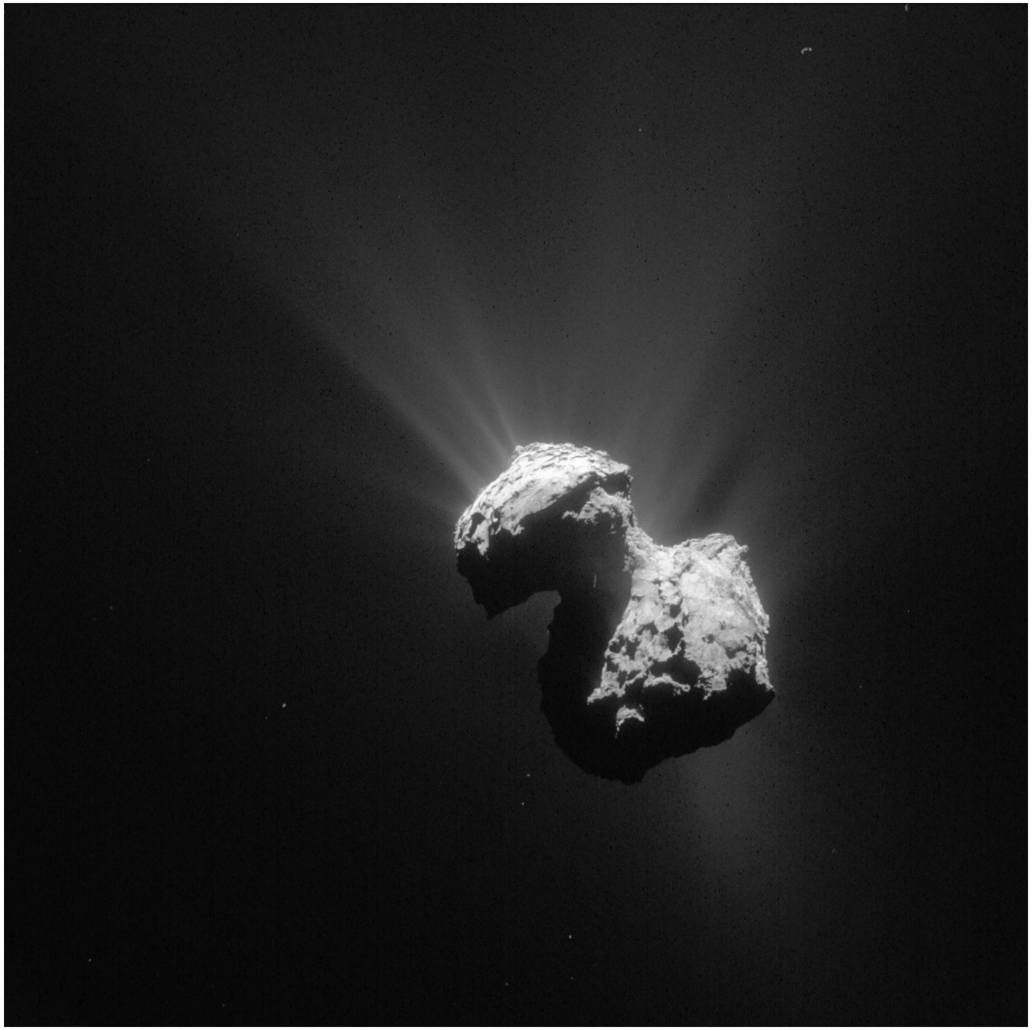

Tchourioumov gerasymenko

~18_{-3} /$^{+81}$ EO

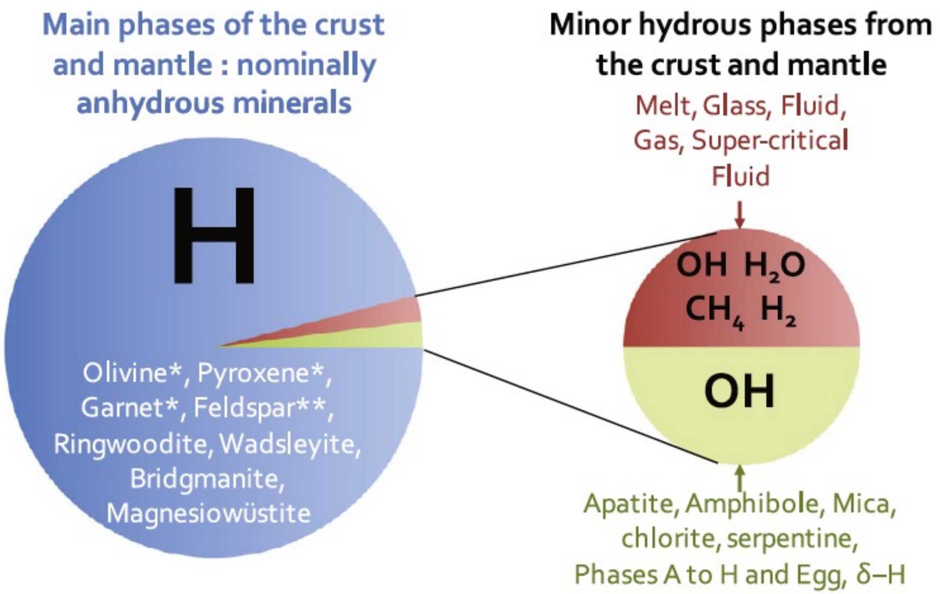

Fig. 1 Sketch illustrating the "water" species present in the various phases of the Earth's mantle and crust. The size of the pie slices represents the approximate volume percentage of the phases. The main reservoir of water in the mantle is nominally anhydrous minerals where hydrogen (H) enters their lattice in defects, and bonds to structural oxygen (*blue field*) (Bell and Rossman 1992b). *Olivine, pyroxene and garnet can incorporate water as H_2 under reduced conditions (Yang et al. 2016). **K-feldspar can sometimes include water as H_2O and NH_4 (Johnson and Rossman 2004)

Peslier et al., 2017

Outline

- Introduction / constraints
- Heat and volatile transfer during MO Phase
- Examples, results and applications to exo-planets

Heat and volatile transfer during Magma Ocean Phase

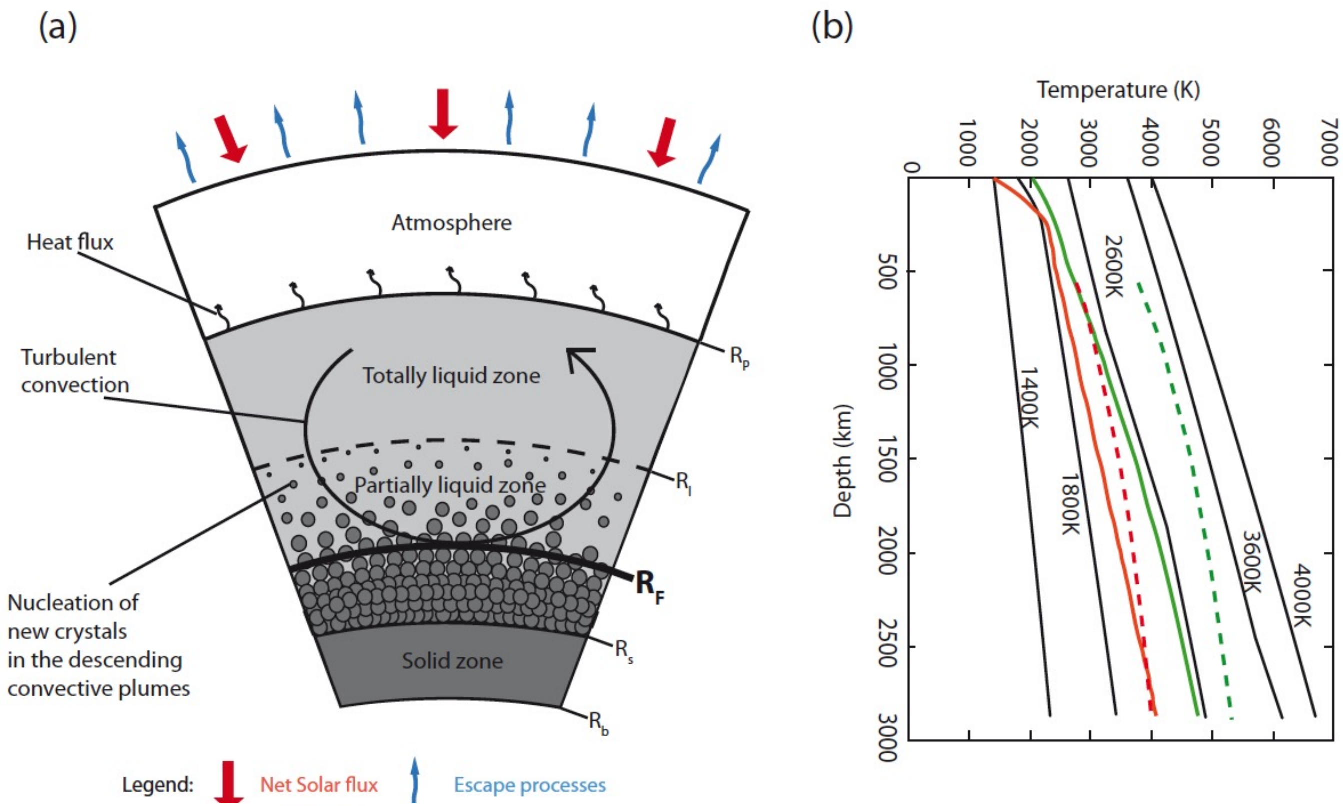

$$SC = \int_{R_b}^{R_p} \rho C_p \frac{dT_p}{dt} r^2 dr = R_P^2 Q_S + R_B^2 Q_B + H_{int} + H_{sol}.$$

Massol et al., 2016

Coupled model

ATMOSPHERE

- Radiative-convective (Marcq, 2012&2017)
- 1D Plan parallel

Heat and volatile transfer

MANTLE

- Parameterized convection, $F_{conv} \propto Ra^{1/3}$
- Bottom up solidification

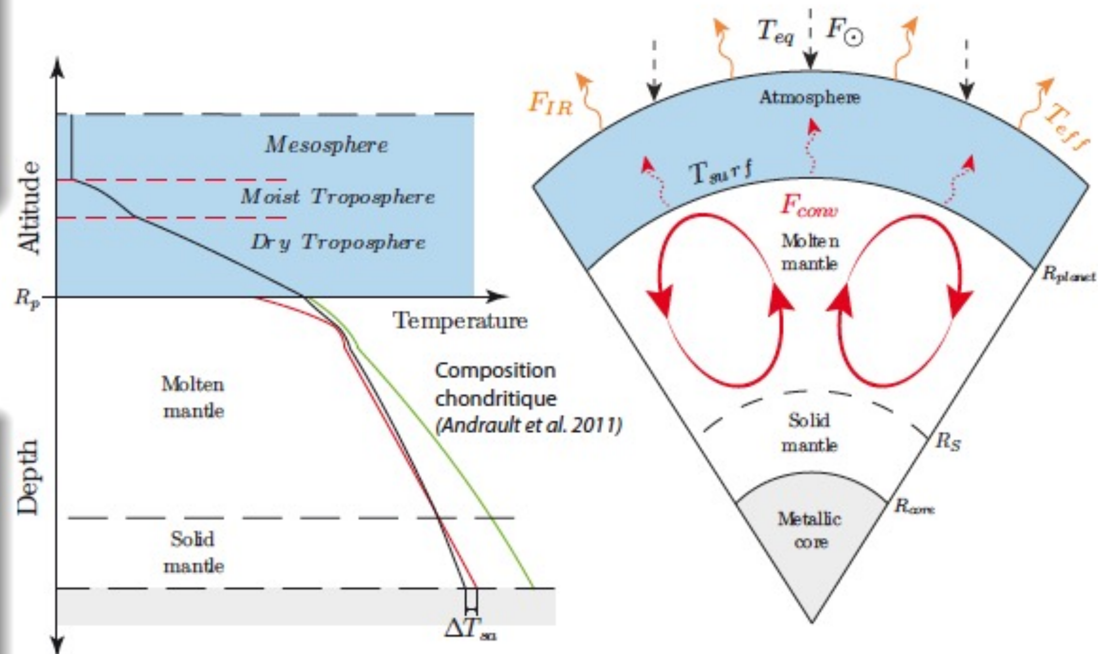

Salvador et al., 2017

Heat and volatile transfer during Magma Ocean Phase: Ra

$u \equiv 0 \qquad \bar{\rho} = \rho_0 (1 + \beta z)$

Statically stable — Statically unstable

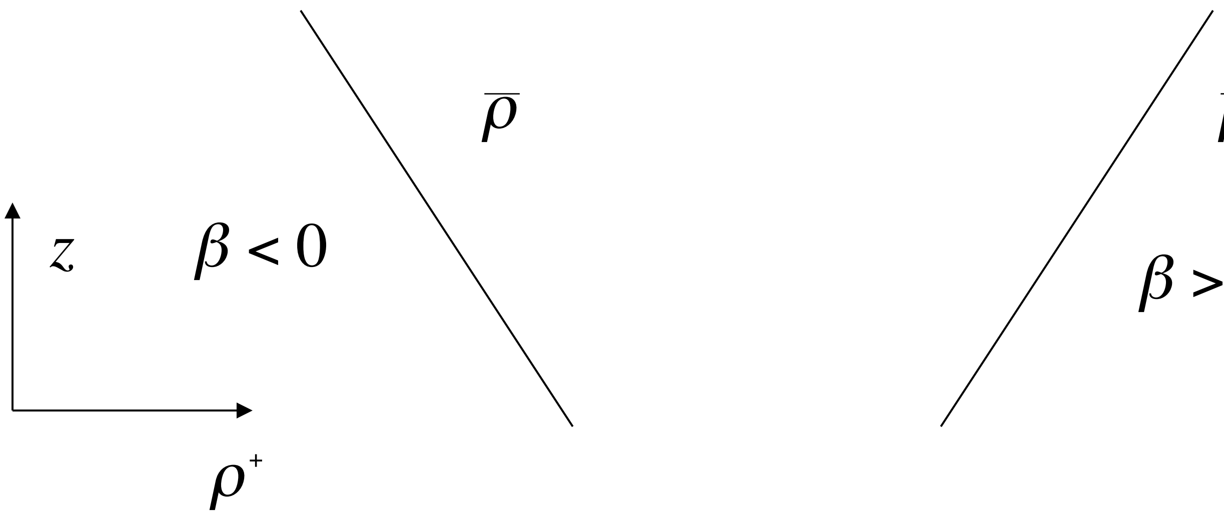

Important physical parameters:	g	ν	κ	β
Dimensions	LT^{-2}	L^2T^{-1}	L^2T^{-1}	L^{-1}

Heat and volatile transfer during Magma Ocean Phase: Ra

Spherical particle of radius h
Displaced upward of h in a time τ

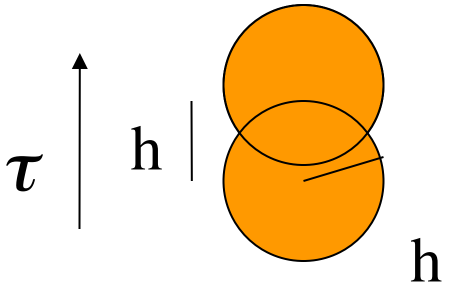

Heat and volatile transfer during Magma Ocean Phase: Ra

-Characteristic velocity **U**?

-Potential energy gained **E**?

-How much **time** for the particle to lose buoyancy?

- What is the **energy D** dissipated by viscous forces?

Heat and volatile transfer during Magma Ocean Phase: Ra

Characteristic velocity : $U \propto \dfrac{h}{\tau}$

Potential energy gained :
$$E \propto (\Delta\rho h^3) gh \propto \rho_0 \beta h h^3 gh \propto \rho_0 \beta g h^5$$

The particle lose buoyancy in a time: $\tau \propto \dfrac{h^2}{\kappa}$

Energy D dissipated by viscous forces : $D \propto \mu \dfrac{U}{h} h^2 h \propto \mu \dfrac{h^3}{\tau} \propto \mu\kappa h$

Instability if E>D → $\rho_0 \beta g h^5 > \mu\kappa h$ i.e.: $Ra = \dfrac{\beta g h^4}{\kappa\nu} > 1$

Convective patterns as a function of Rayleigh number:

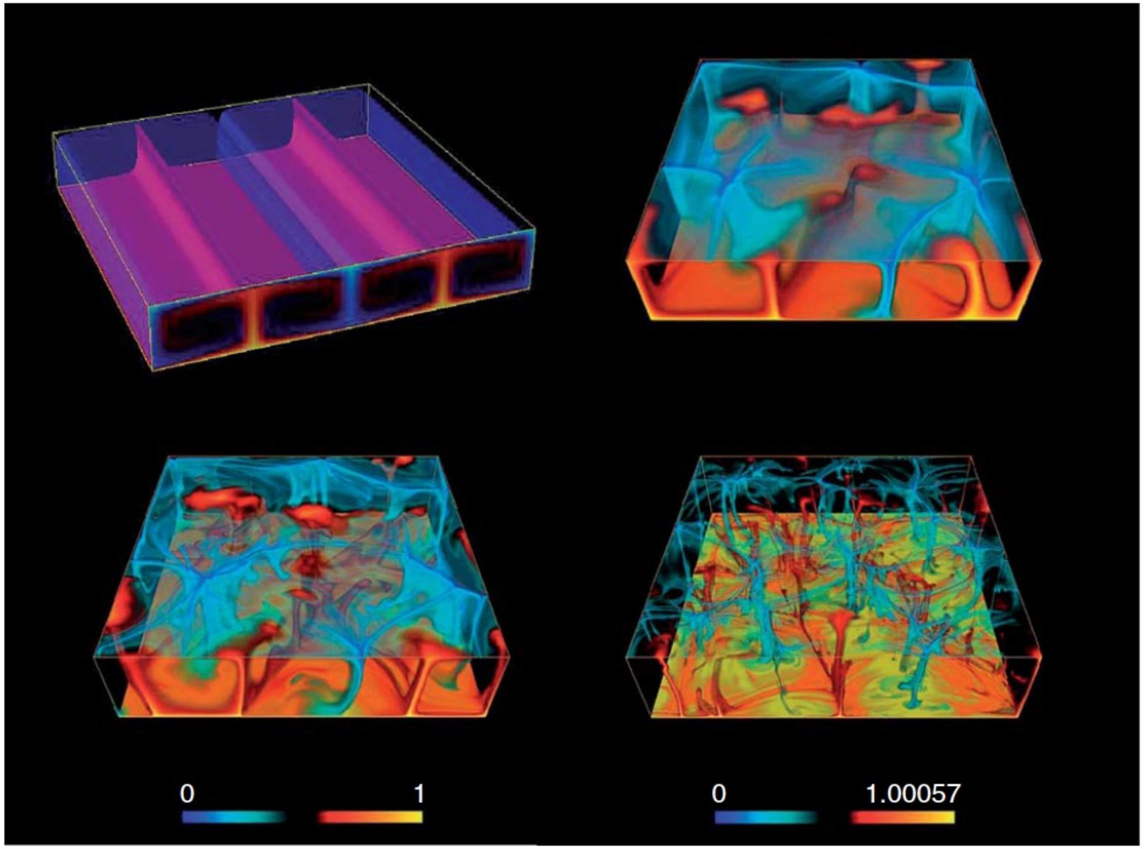

with $\beta = \frac{\alpha \Delta T}{h}$

$$Ra = \frac{\alpha g \Delta T h^3}{\kappa \nu}$$

up to Ra=30 for entirely liquid MO

Figure 4 Convection patterns of a fluid heated from below at Rayleigh number 10^5, 10^6, 10^7, 10^8. The temperature color bars range from 0 (top boundary) to 1 (bottom boundary). The Boussinesq approximation was used (numerical simulations by F. Dubuffet). The increase in Rayleigh number corresponds to a decrease of the boundary layer thicknesses and the width of plumes. Only in the case of the lowest Rayleigh number (top left) is the convection stationary with cells of aspect ratio $\sim \sqrt{2}$ as predicted by marginal stability. For higher Rayleigh number, the patterns are highly time dependent.

Ricard, 2007

Viscosity

After Takei and Holtzmann 2009

Interpolation between η_s (Karato et Wu, 1993) et η_l (Karki et Stixrude, 2010)

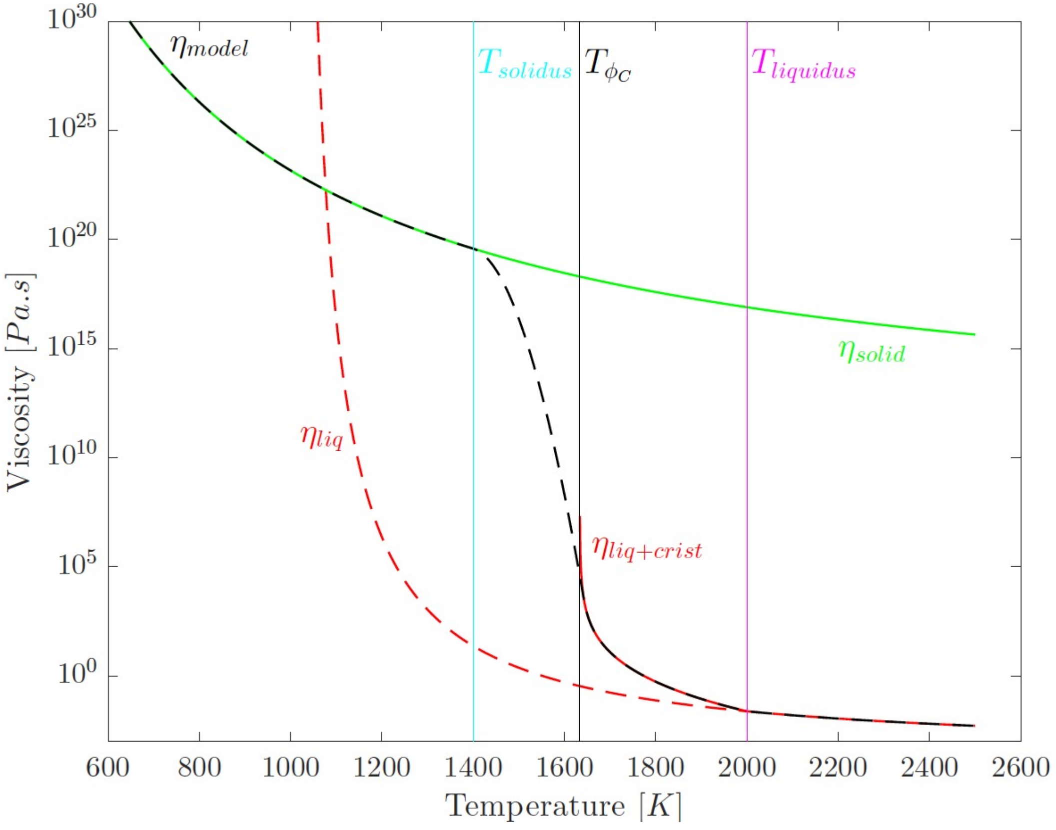

Salvador et al., 2017

Heat and volatile transfer during Magma Ocean Phase

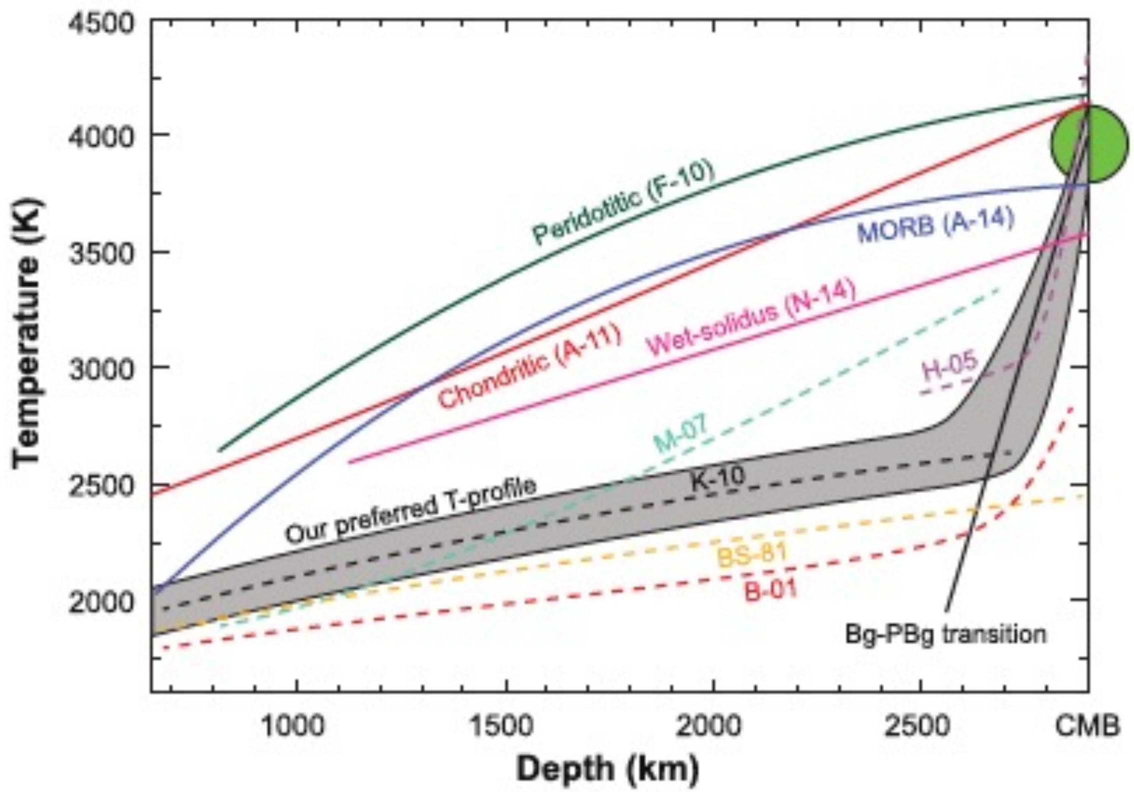

Andrault et al., 2016

Exsolution

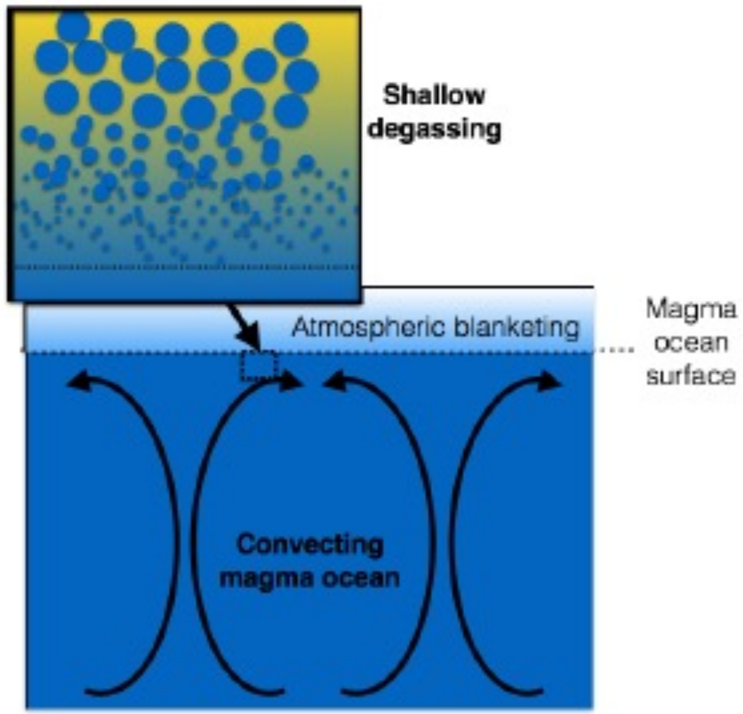

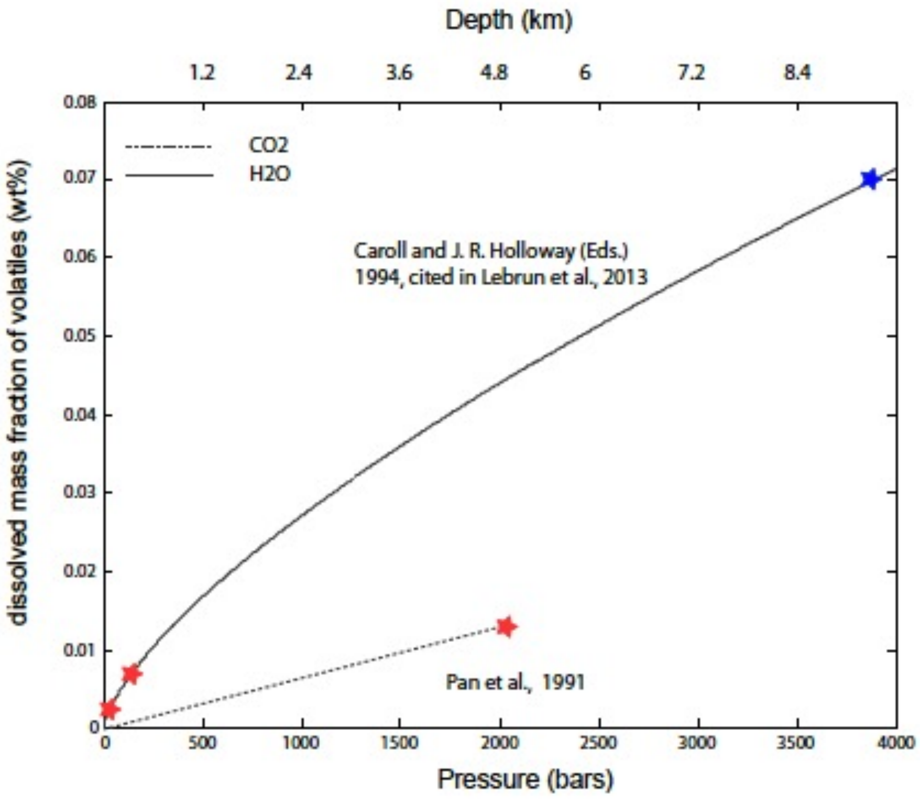

More references in Iacono et al., 2012

Mass conservation of volatiles

$$M_{vol}^{\text{solid}} + M_{vol}^{\text{liquid}} + M_{vol}^{\text{atm}} = X_{vol,t=0} M_{t=0}^{\text{MO}}$$

$$M_{vol}^{\text{atm}} = \frac{4\pi R_p^2}{g} \left(\frac{\mu_{vol}}{\bar{\mu}}\right) P_{vol}(X_{vol}^{\text{liquid}})$$

Heat and volatile transfer during Magma Ocean Phase: Ra

Definition: End of Rapid Cooling Stage

- Limit between two evolution stages:
  - Controlled by F_{conv}, vigorous mantle convection, strong cooling, degassing of the atmosphere
  - Controlled by $F_{\odot}$, quasi steady-state: T_{surf} and P_{atm}, other geodynamic regime
- ERCS taken at time when $F_{conv} = \frac{1}{10} F \odot$

Outline

- Introduction / constraints
- Heat and volatile transfer during MO Phase
- Examples, results and applications to exo-planets

Time evolution

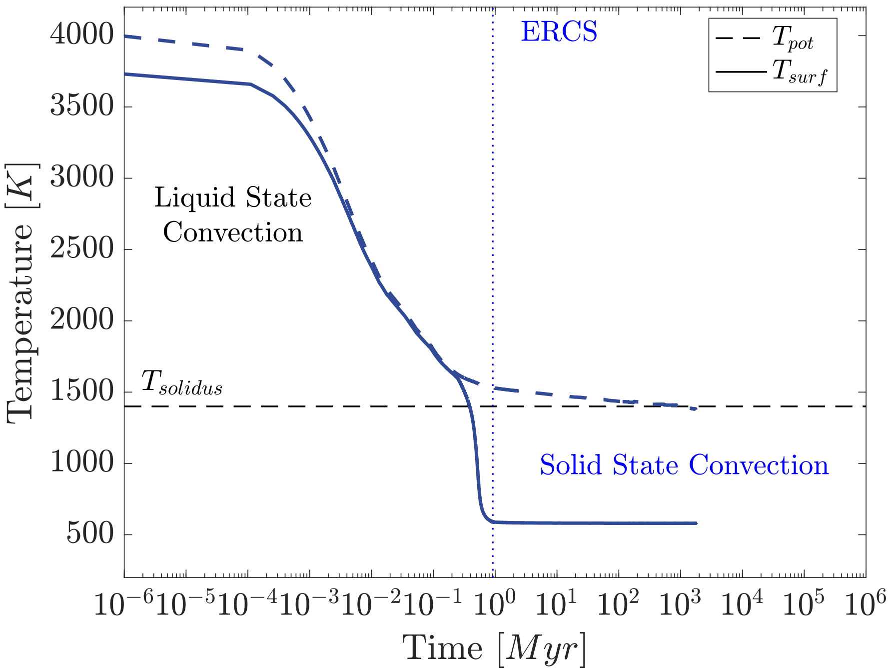

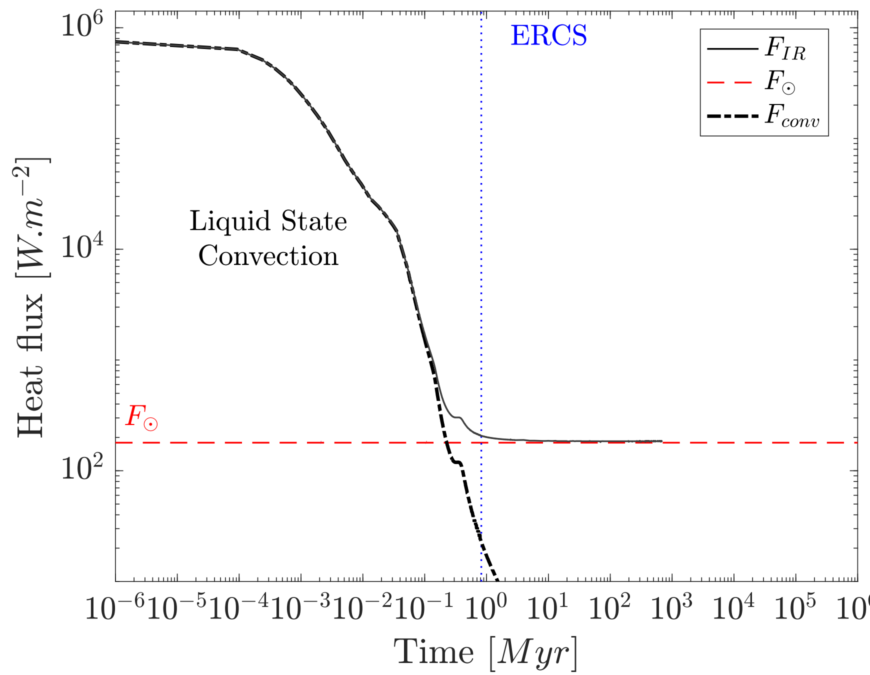

$CO_{2:}$ 600 ppm; H_20: 0.4 EO; D=1 AU α=0.2

Degassing

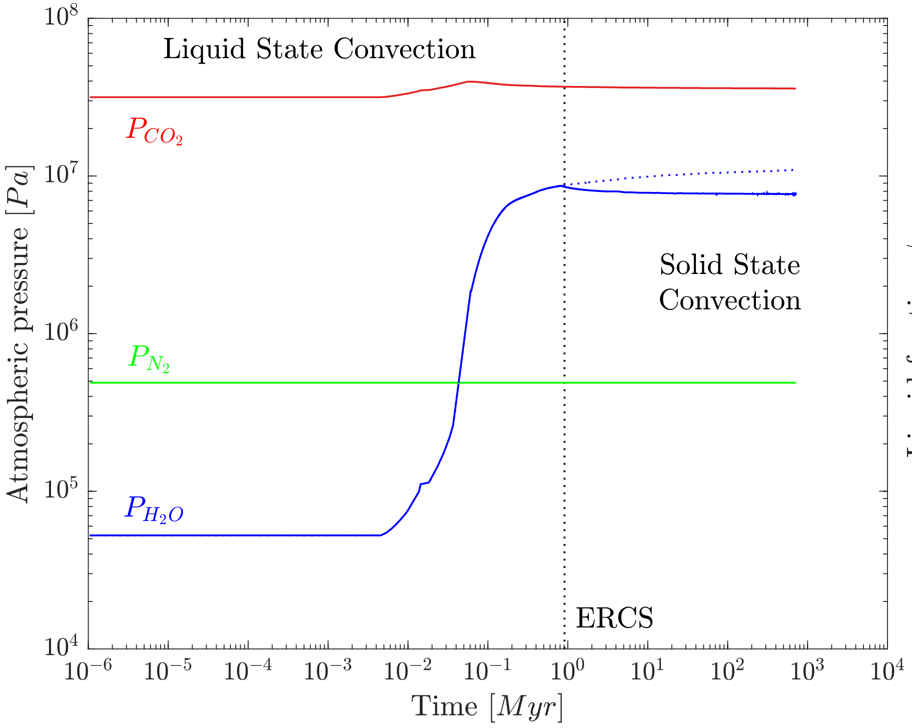

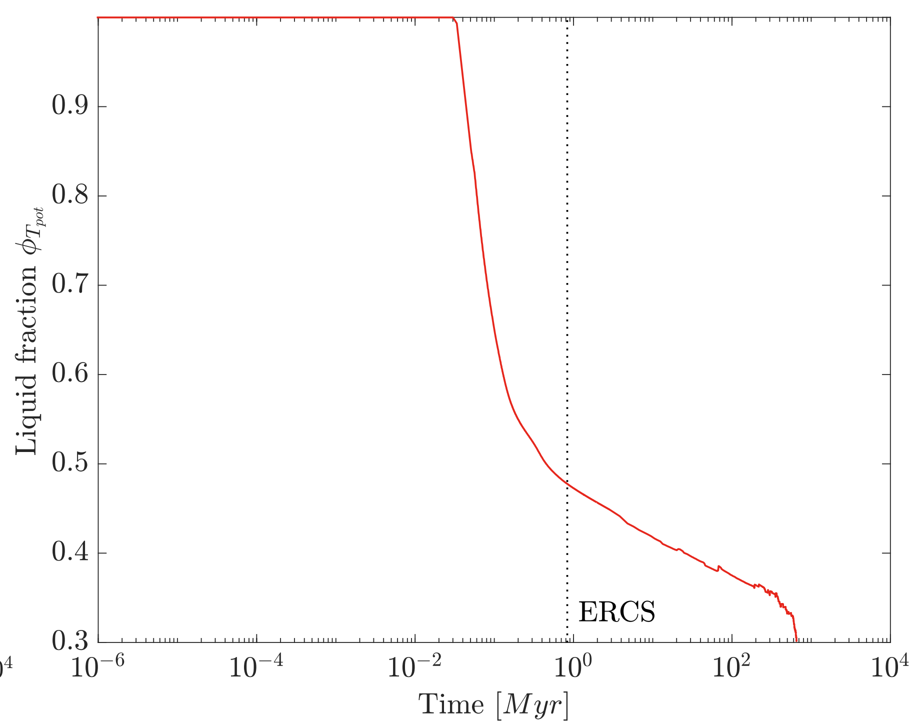

CO_2: 600 ppm; H_20: 0.4 EO; D=1 AU α=0.2

Examples, results and applications

Distance to the sun

0,77

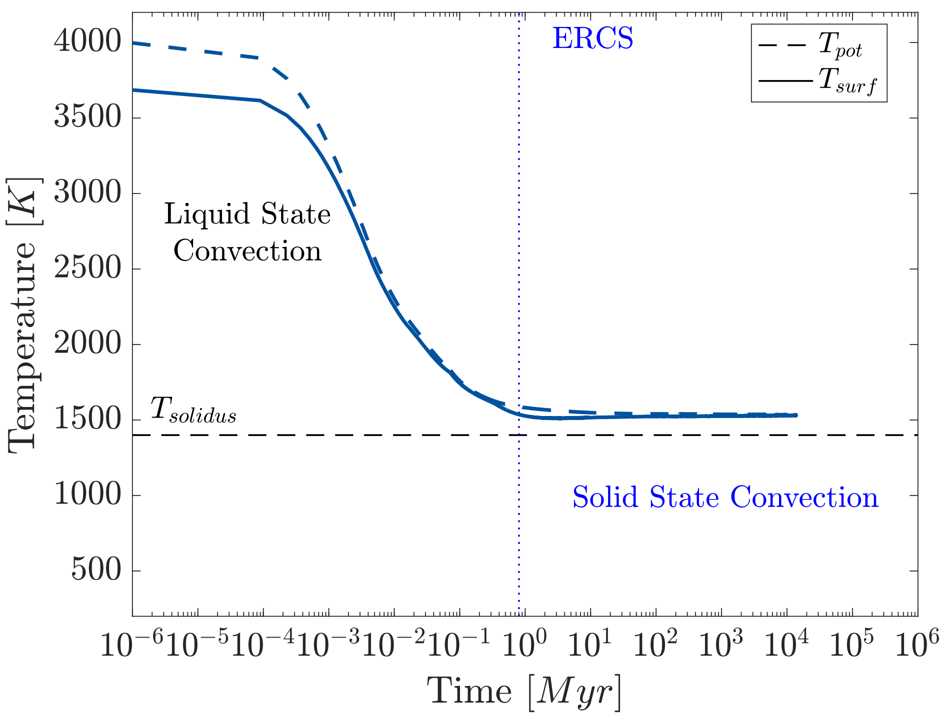

1,3

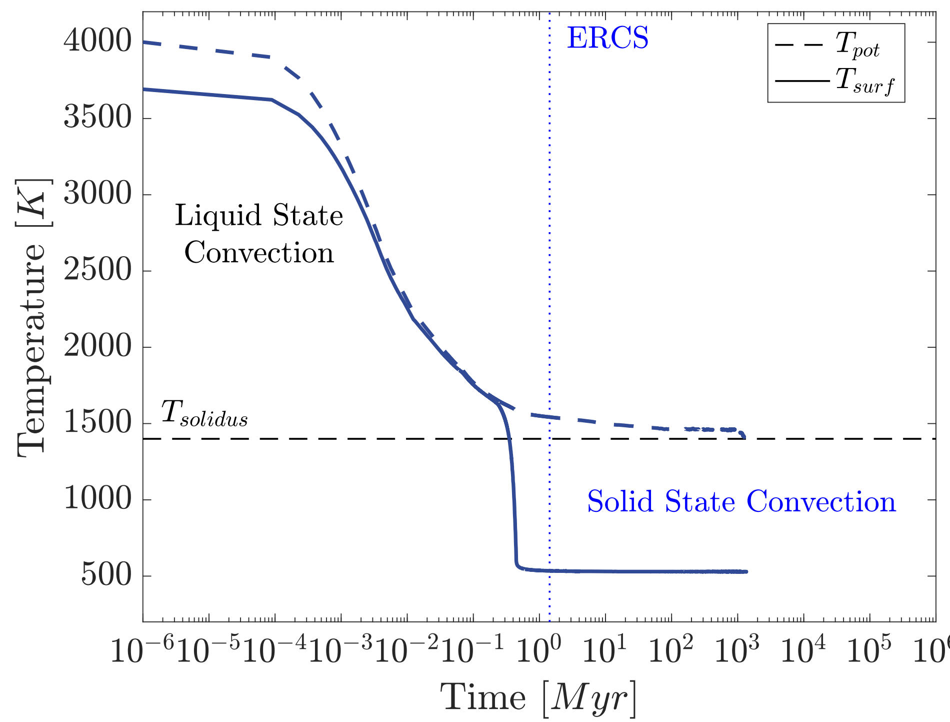

End of Rapid Cooling Stage

ERCS : $F_{conv} \leq 0.1 \times F_{\odot}$

Volatiles

$H_2O = 0.6$ MEO, $CO_2 = 500$ ppm

CO_2 content

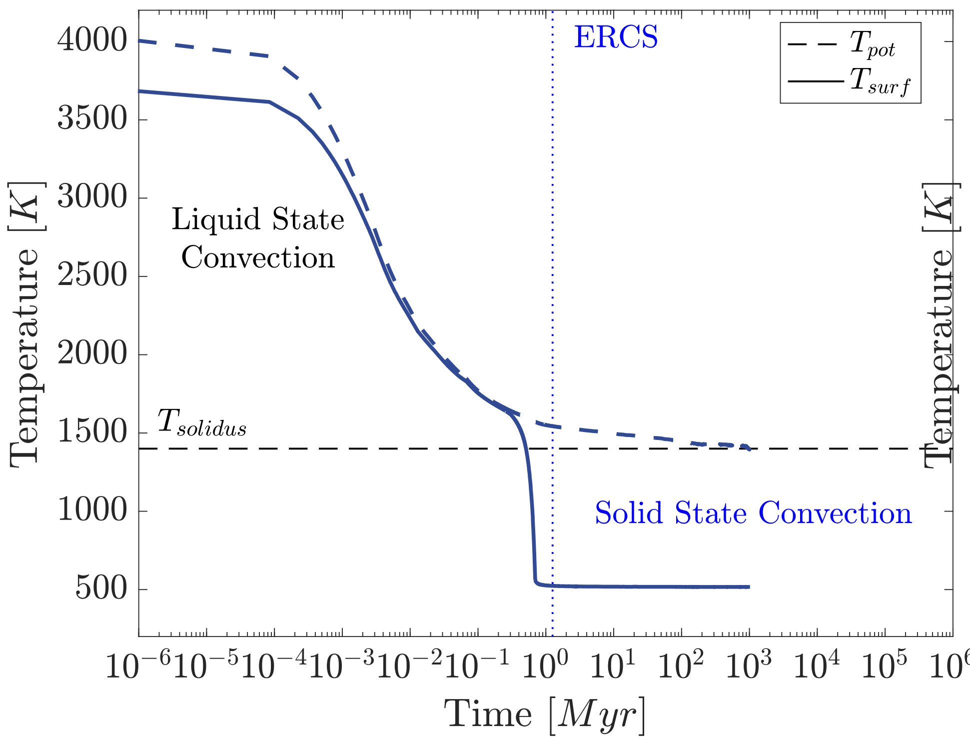

CO_2: 400 ppm; H_20: 0.6 EO; D=1 AU α=0.2

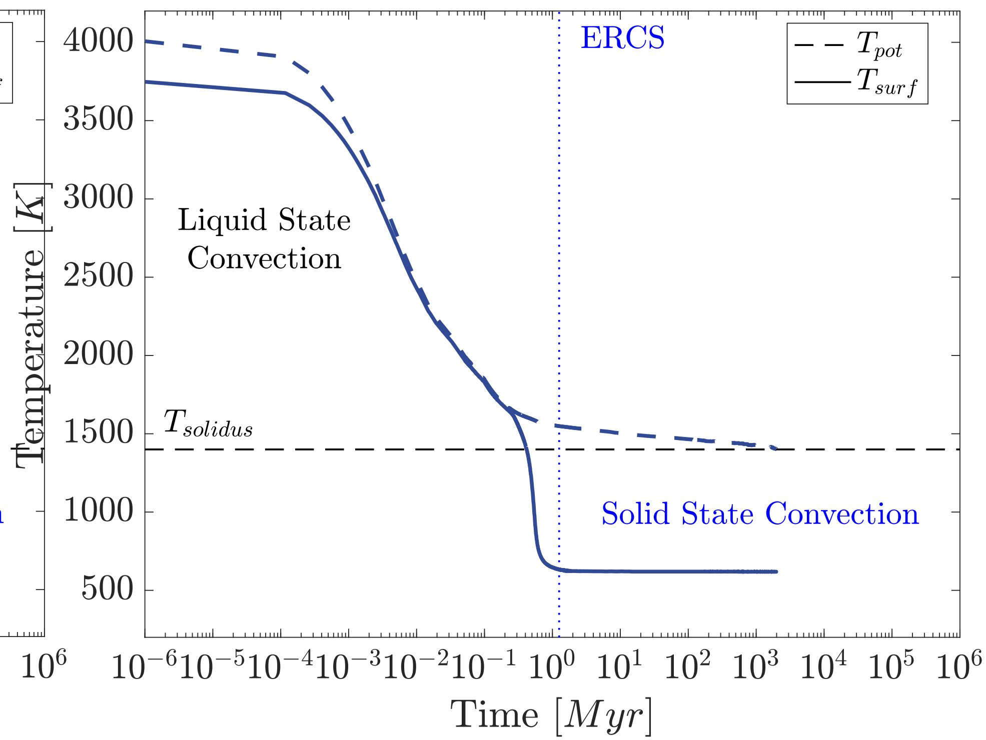

CO_2: 1200 ppm; H_20: 0.6 EO; D=1 AU α=0.2

$H_2O = 0.6$ MEO, $\alpha = 0.2$

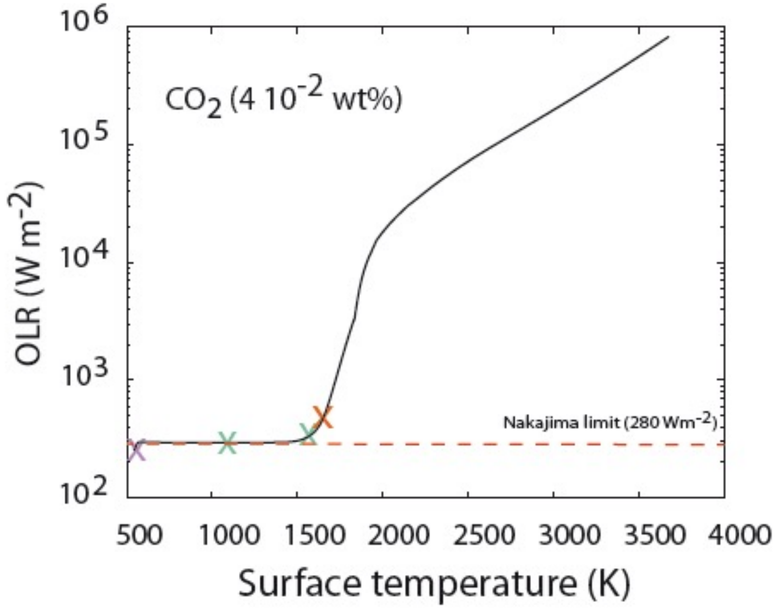

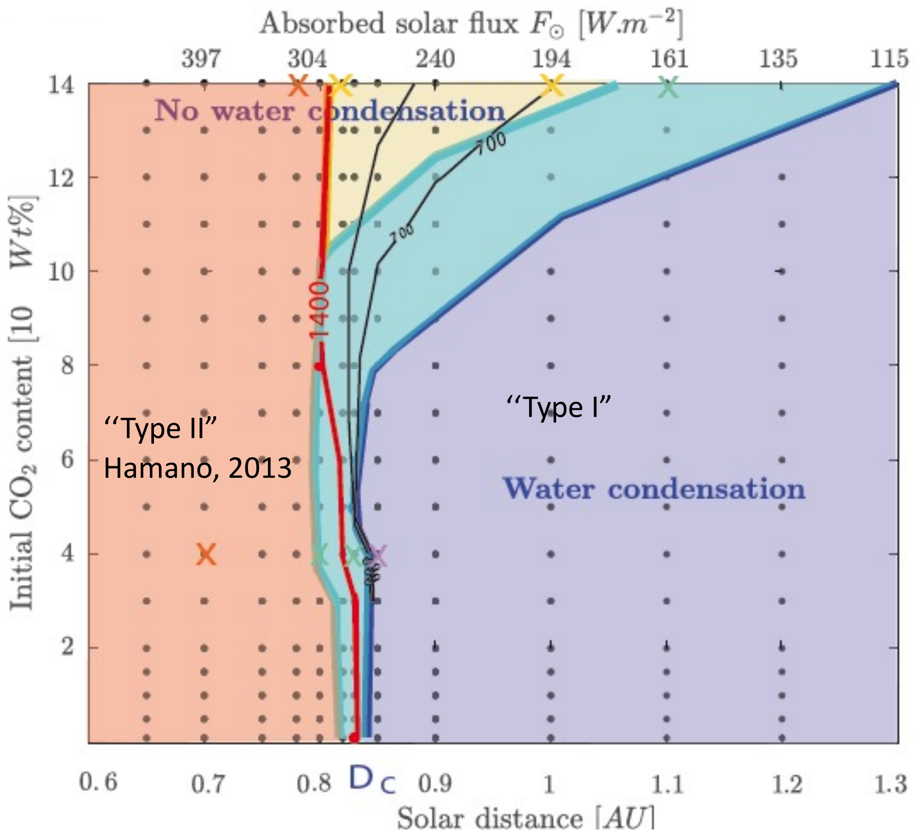

- partial melt
- no condensation
- condensation post ERCS
- condensation at ERCS

For different initial water content

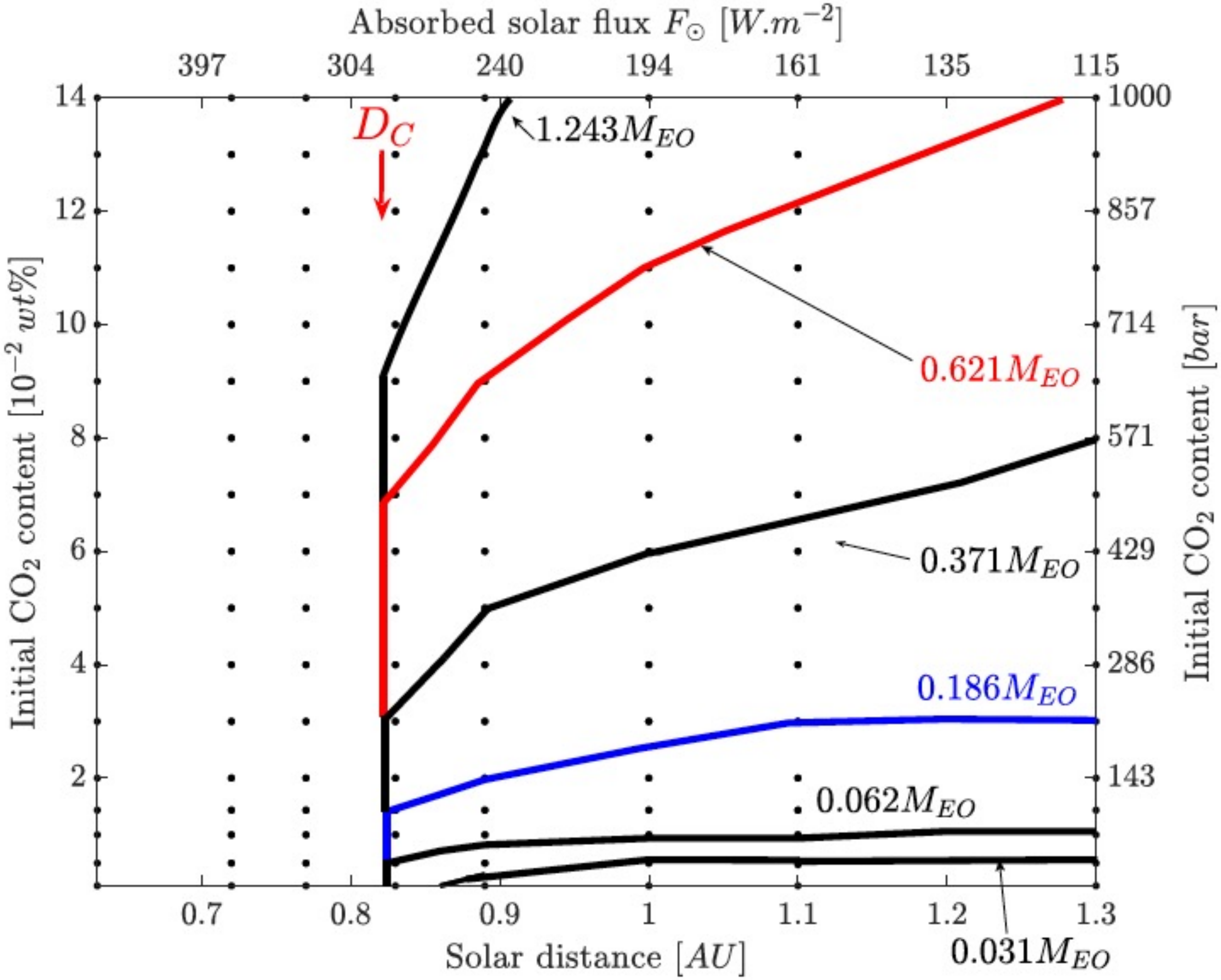

Scaling

volatiles

$$x^* = \frac{x[0]_{CO_2}}{x[0]_{CO_2} + x[0]_{H_2O}}$$

Distance to the star

$$D_C = \sqrt{\frac{F_0(1-\alpha)}{F_{IR}}}$$

F_O being the solar constant for the young sun and F_{IR} the Nakajima limit (280 W m^{-2} In Marcq et al. model used here)

$$D^* = \frac{D}{D_C} = 0.814$$

Venus

For a 0.4 albedo it requires 0.13 Earth Ocean ($x^* \approx 0.65$)

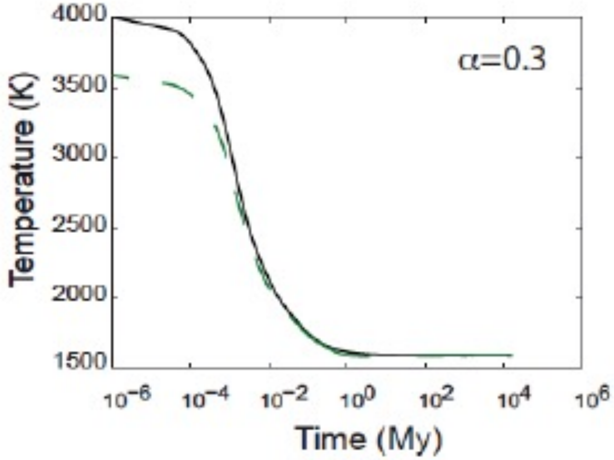

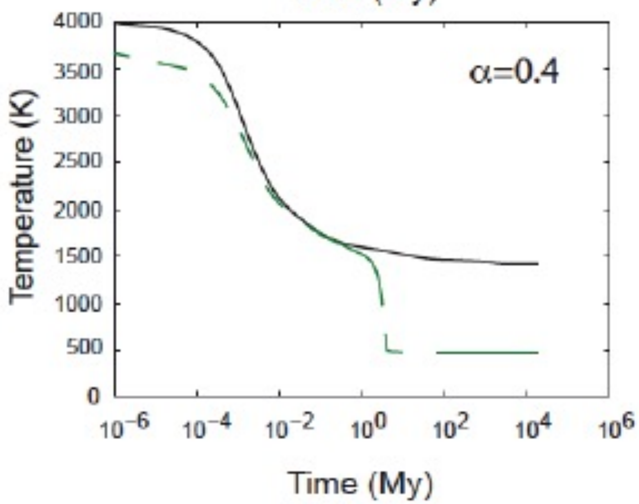

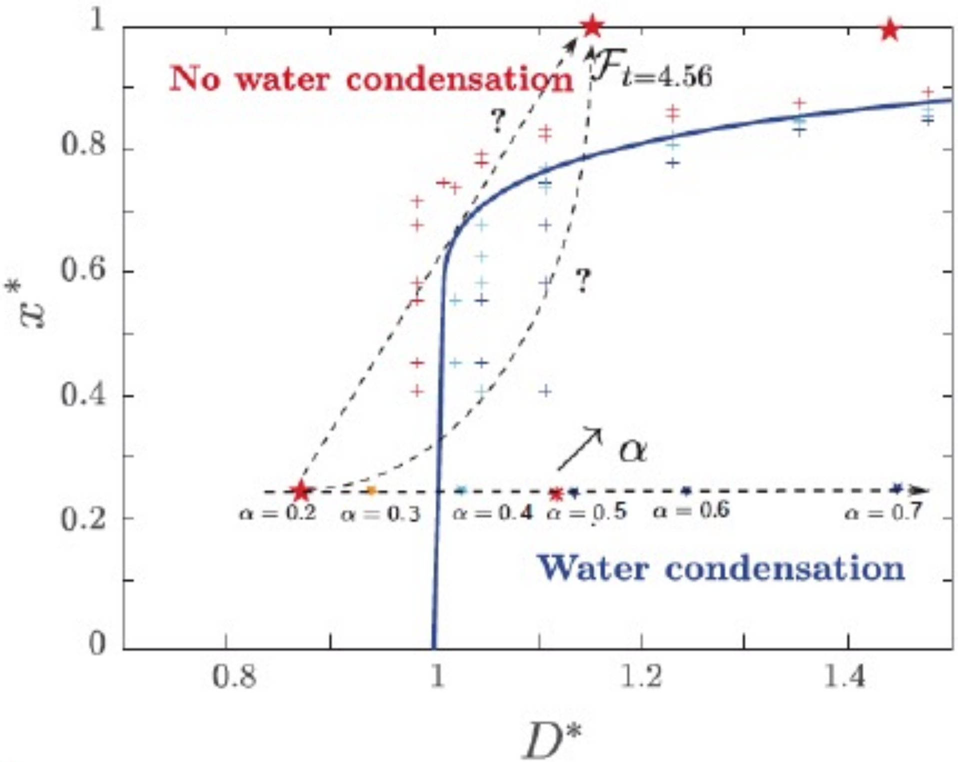

Examples, results and applications

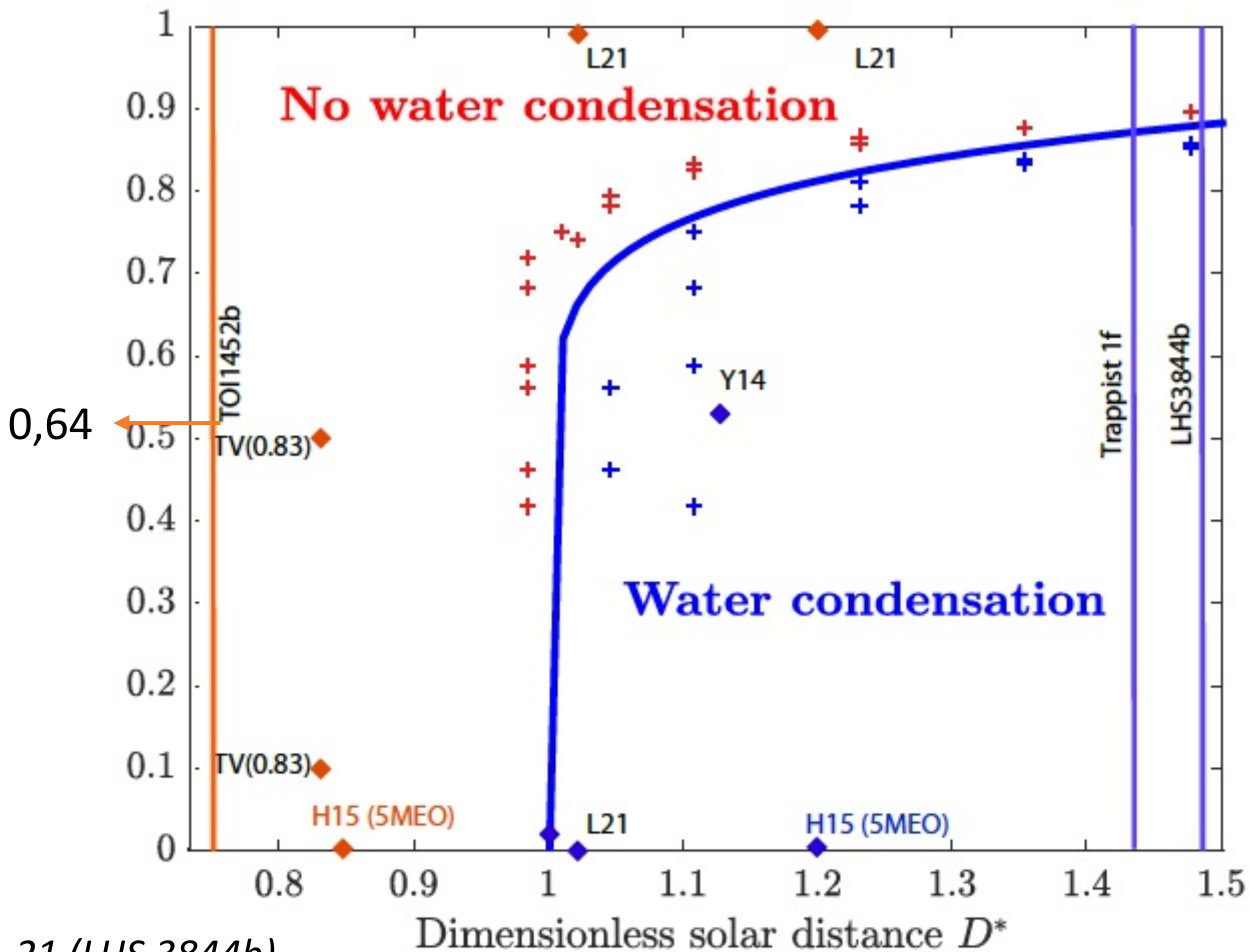

Meier, 21 (LHS 3844b)

Dorn and Lichtenberg, 21 (Trappist 1f)

Cadieux, 22 (TOI1452b)

Massol et al. in prep.

Perspectives:

- Post MO Heat and volatile transfer
- Surface conditions and fracturation

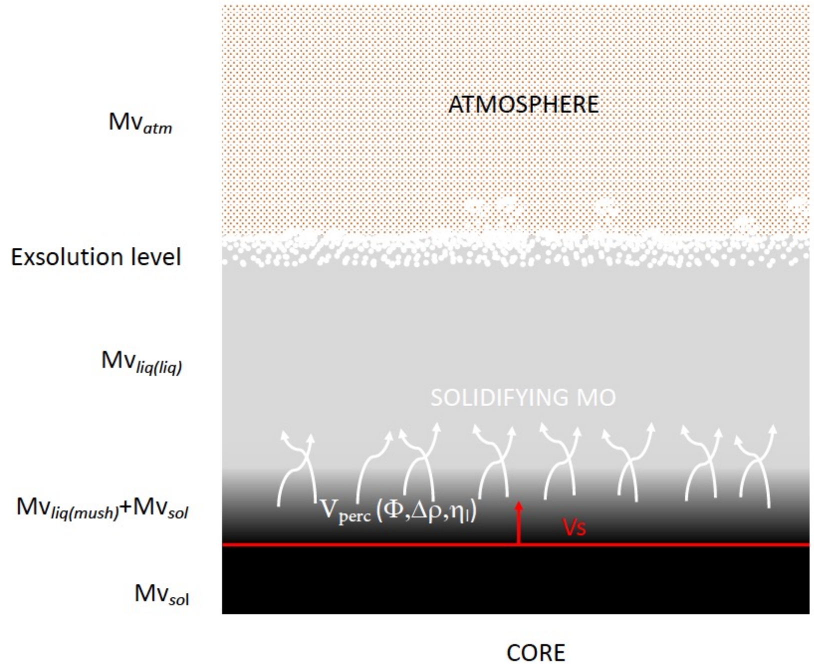

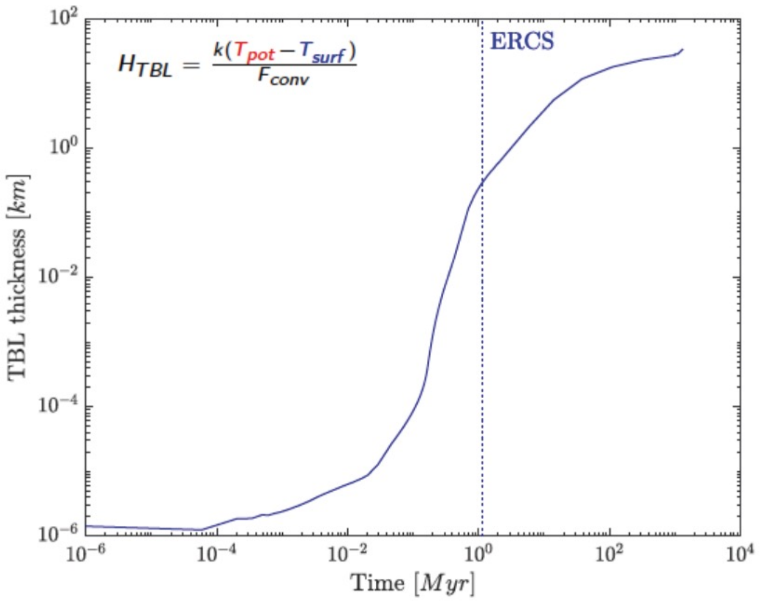

Application to exoplanets: remarks, questions?